# Arsenic removal by adsorption on activated carbon in a rotating packed bed

Mohd Ali Hashim[a][1], Anirban Kundu[b], Sumona Mukherjee[b], Yee-Sern Ng [c][*], Soumyadeep Mukhopadhyay[d][*], Ghufran Redzwan[b], Bhaskar Sen Gupta[e]

[a]  Department of Chemical Engineering, University of Malaya, 50603, Kuala Lumpur, Malaysia

[b]  Institute of Biological Sciences, University of Malaya, 50603, Kuala Lumpur, Malaysia

[c]  Department of Chemical Engineering, Lee Kong Chian Faculty of Engineering & Science, Universiti Tunku Abdul Rahman, Jalan Sungai Long, Bandar Sungai Long, 43000 Kajang, Selangor, Malaysia

[d]  Scientific Event Ltd, 31, Cannon Street, Seton Park, Winchburgh, Broxburn, EH52 6WN, Scotland, UK

[e]  Water Academy, Institute of Infrastructure and Environment, Heriot-Watt University, Edinburgh Campus, EH14 4AS Scotland

*  Previous affiliation: Department of Chemical Engineering, University of Malaya, 50603, Kuala Lumpur, Malaysia


[1] *Corresponding Author*

Mohd Ali Hashim

Department of Chemical Engineering, University of Malaya, 50603, Kuala Lumpur, Malaysia

Tel: +603-79675296

**Email :** alihashim@um.edu.my

**Abstract**

High gravimetric technology or HIGEE is a novel technique which uses centrifugal force in a rotating

packed bed (RPB) contactor. In RPB, a doughnut shaped bed is spun at high speed to allow fluid to

flow through an adsorbent bed at a high velocity.  Centrifugal force enhances the adsorption process

with increased mass transfer coefficient. In this study, the optimum condition of the working

parameters of a RPB contactor for arsenic removal by activated carbon was investigated and

optimized by Taguchi method. Five parameters, namely rotating speed, feed rate, packing density,

initial concentration and initial solution pH were considered in determining the initial optimal

condition in a L16 orthogonal array. According to the signal to noise ratio (S/N), the optimum

condition obtained from the L16 experiments are rotating speed of 1600 rpm, feed rate of 50 L/h,

packing density of 510 kg/m$^3$, initial concentration of 150 mg/L and pH of 3. Depending upon the

delta value, which is the difference between the highest and lowest S/N ratio, it was found that the

initial concentration was the least affecting factor and pH could be fixed at 3 for practical purposes.

# 1 Introduction

Enhancement of mass transfer by using centrifugal force field was achieved through the innovation of high gravimetric technology (HIGEE) in the late 1970s at ICI. The mass transfer process is carried out in a doughnut shaped bed known as a rotating packed bed (RPB) (Stankiewicz and Moulijn, 2000). As mentioned by Lin and Liu (1999), RPB contactor was first designed by Collin Ramshaw and Roger H. Mallinson in the year 1981 for effective mass transfer process between two fluid phases. This doughnut shaped bed is spun at high speed to achieve high centrifugal force. Due to the elevated force, very thin liquid films and/or tiny droplets are created in the packing area. Thus, gas-liquid or liquid-liquid or solid-liquid interfaces are constantly renewed, which aid in considerable intensification of mass transfer between the phases (Wang et al., 2008). Initially, these RPB-HIGEE systems were used in separation processes such as distillation and absorption. However, it can also be applied in mass transfer limited reacting systems. The advantages of using HIGEE are: i) higher throughput, and ii) the formation of thinner liquid film over the packings. This results in decreased external mass transfer resistance, higher surface packing per unit volume of packed bed, better distribution of liquid over the packings and lower static holdup. Thus, the size of the processing equipment is significantly reduced in comparison to a conventional packed bed. Moreover, it is likely to reduce the overall cost of wastewater treatment (Lin and Liu, 1999; Ramshaw and Mallinson, 1981). Adsorption, being a mass transfer controlled process, the HIGEE technology in RPB can be used for adsorptive removal of heavy metals or dyes from wastewater.

Adsorption onto activated carbon is one of the most effective methods for heavy metal removal. However, the size of an industrial facility is generally large to facilitate the high volume of effluent. Due to the high throughput, the RPB-HIGEE can be useful in treating high volume of wastewater. Lin and Liu (1999) studied the adsorption of Basic Yellow 2 dye on activated carbon in a centrifugal adsorption bed influenced by centrifugal acceleration whilst Das et al. (2008) experienced enhanced volumetric mass transfer coefficient for biosorption of Cu(II) ions on *Catlacatla* fish scale with increasing rotor speed in RPB contactor. Panda et al. (2011) also reported better mass transfer rate at higher rotational speed while using crude tamarind (*Tamarindus indica*) fruit shell to remove

Cr(VI) ions from an aqueous solution in a RPB contactor. In the present work, we have extended the investigation for one of the most toxic elements, which is arsenic (As).

Arsenic is reported to be one of the most toxic heavy metals that can exist in the water body. Arsenic occurs naturally in soils and can be mobilized by weathering reactions and biological activities and this may lead to contamination of surface or groundwater aquifers (Wang et al., 2015). Elevated levels of arsenic in groundwater have been reported in many countries, such as Chile, Mexico, China, Argentina, USA, Hungary, India (West Bengal), Bangladesh and Vietnam (Shankar et al., 2014). The consumption of water with high arsenic content can cause several acute and chronic illnesses such as nausea, abdominal pain, diarrhea, multisystem diseases besides inactivating up the enzymes that are involved in cellular energy pathways and DNA synthesis and repair (Ratnaike, 2003). Arsenic poisoning is also reported to cause skin lesions and cancer of the liver, brain, stomach and kidney (Roghani et al., 2016). Due to the fact that drinking water is one of the major routes for arsenic uptake, a very strict drinking water allowance limit of 10 μg/L has been prescribed by the US Environmental Protection Agency (USEPA, 2017). Nevertheless, it is worth noting that the mobility of arsenic is dependent on its species and valence state. Under aerobic environments, As(V) is dominant, usually in the form of arsenate $(AsO_4)^{3-}$. Under reducing conditions, As(III) dominates, existing as arsenite $(AsO_3)^{3-}$ which is water soluble and is 25-60 times more toxic than As(V) (Korte and Fernando, 1991; Roghani et al., 2016). Recently, there have been a number of publications reporting technologies that can effectively remove arsenic from water, and these are electrocoagulation (Kobya et al., 2011; Banerji and Chaudhari, 2016), electrodialysis (Ortega et al., 2017), and adsorption using iron coated seaweeds (Vieira et al., 2017), magnet-responsive nanomaterials (Nisticò et al., 2018) and magnetic chitosan (Malwal and Gopinath, 2017). However, there is no reported work on the removal of arsenic by activated carbon in RPB contactor. In the present study, an optimization will be performed by Taguchi method to obtain a robust product or process design at low cost. Orthogonal array will be used to determine optimum design points by performing minimum number of experiments (Durán-Jiménez et al., 2014; Taguchi, 1986). The 'log' functions of desired output, defined by Taguchi as Signal-to-Noise ratios (S/N), serve as the objective

4

function for data analysis and optimization (Apte, 2000). Taguchi method also considers the effects of noise factors, which are inconvenient to control. In this method, the optimum condition will be insensitive to the noise factor.

The specific objective of the present work is to employ activated carbon in RPB contactor system and optimise the process variables that are important for As removal. The operating parameters such as the rotor speed, feed rate, activated carbon packing density, initial concentration and initial pH of the solution were selected for the purpose.

# 2 Materials and Methods

## 2.1 Materials

All chemicals used were of reagent grade. The arsenic species in this study was As(V), which was prepared using $Na_2HAsO_4.7H_2O$. The activated carbon was purchased from Sigma-Aldrich and was used as received.
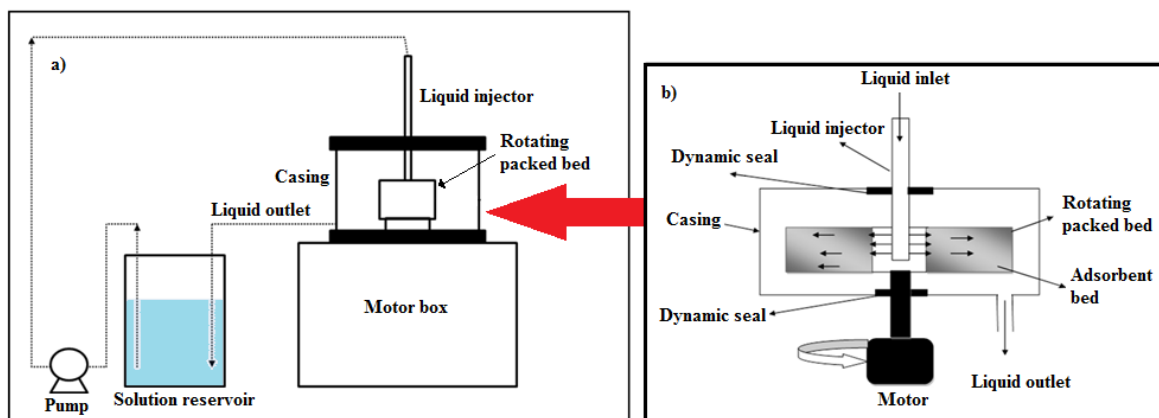
## 2.2 Rotating packed bed system



**Fig. 1:** Schematic diagram for a) the experimental setup, and b) rotating packed bed contactor

A RPB reactor is a special type of contactor in which a doughnut shaped packed bed is rotated using a motor, as shown in Fig. 1. The height of the RPB is 2.5 cm. The inner radius of the rotor is 2 cm and the outer radius is 3.2 cm. The annular space for the packing is 1 cm width. The inner and outer walls are made of stainless steel mesh of size 50 µm. The rotor is driven by a 0.5 hp motor at a speed ranging from 100 to 2000 rpm, thereby generating 0.3 to 112 times the gravitational force on the basis of the arithmetic mean radius. The activated carbon was placed in the annular space of the rotor at various packing densities. Arsenic solution was injected through a port on the inner wall of the rotor, coming out from the outer wall of the rotating rotor. The liquid flow path is as indicated in Fig. 1b.

## 2.3    Taguchi method

In Taguchi method, a set of response variables are tested against a set of control parameters or independent variables by experiments arranged in "orthogonal array" to obtain the most suitable combination of the control parameters. Orthogonal arrays provide a best set of well-balanced and minimum number of experiments required to identify the optimum conditions. The log functions of desired outputs, which are known as the signal to noise ratios (S/N), serve as the objective functions for optimization. The S/N ratio is also used in data analysis and in the prediction of the optimum results. The target of a process as defined here is the numerical value that is preferred for the quality characteristic of interest. Depending upon the target value, there are three forms of S/N ratios, namely: i) smaller-the-better, ii) larger-the-better, and iii) nominal-the-best, which are of common interest for optimization of static problems expressed by Equations 1, 2 and 3, respectively, where S/N is the S/N ratio, R is the percentage removal at each run, n is number of repeated runs for each experiment, and $\sigma$ is the standard deviation. In the present work, the algorithm for larger-the-better S/N ratio was chosen for the optimization as the removal of arsenic should be as high as possible at the optimum condition (Aber et al., 2009; Li et al., 2010).

$$\frac{S}{N} = -10\log\left(\frac{1}{n}\sum_{i=1}^{n}R_i^2\right) \qquad (1)$$

$$\frac{S}{N} = -10\log\left(\frac{1}{n}\sum_{i=1}^{n}\frac{1}{R_i^2}\right) \qquad (2)$$

$$\frac{S}{N} = 10\log\left(\frac{\overline{R^2}}{\sigma^2}\right) \qquad (3)$$

The optimization process was carried out in two stages. At the initial stage, which can be taken as the coarse optimization, the full possible range was considered for each of the control factors that are important for the removal of arsenic. In this stage, the significance and contribution of the factors towards the optimization were identified. However, as the levels chosen at this stage were of very wide range, the optimum point obtained might not be very accurate. Thus, in the second stage, which can be taken as the fine-tuning stage, the levels chosen were in close vicinity to the initial optimum points. Thereby, a more accurate optimum point was derived.

### 2.3.1    Initial determination of best settings (Coarse optimization)

An L16 orthogonal array was chosen for the initial determination of the best settings, where 16 different experiments were carried out. The experiments were performed with different combination of rotating speed, feed rate, packing density, initial concentration and initial solution pH. The levels and range for each parameter are illustrated in Table 1. As the arsenic species employed was arsenic (V), the pH range selected was 2-5. This is based on previous experiments which state that arsenic(V) is favoured to be adsorbed on activated carbon at low pH range(Chuang et al., 2005; Mondal et al., 2013; Gupta and Chen, 1978; Wei et al., 2016). In addition, the feed rate and packing density were selected based on the operating limitation of the set-up. The feed rate was investigated within the range 20-50 L/h as 50 L/h was the maximum possible operating condition for the peristaltic pump. The range of packing density was $153 - 510$ kg/m$^3$ based on the mass of activated carbon that can be

positioned in the RPB contactor. At maximum mass of the activated carbon, the packing density was 663 kg/m$^3$, which was investigated during the fine-tuning experiments.

**Table 1:** Levels of the control factors for coarse optimization.

| Investigating parameters | Level 1 | Level 2 | Level 3 | Level 4 |
|---|---|---|---|---|
| Rotating speed (rpm) | 400 | 800 | 1200 | 1600 |
| Feed rate (L/h) | 20 | 30 | 40 | 50 |
| Packing density (kg/m$^3$) | 153 | 255 | 357 | 510 |
| Initial solution pH | 2 | 3 | 4 | 5 |
| Initial concentration of As (mg/L) | 50 | 100 | 150 | 200 |

The experimental design matrix of L16 array that is suggested by the Taguchi method is given in Table 2. In the experiment, activated carbon was packed in the annular space of the rotor at different packing densities as specified in Table 2. For each run, 1 L of arsenic solution of desired concentration was taken in a 2 L beaker serving as the reservoir. The solution was recirculated from the reservoir by a peristaltic pump capable of maintaining the flow rate required for that particular run. The system ran for one hour and then a final sample was drawn from the reservoir for testing final arsenic concentration using Inductive Coupled Plasma-Optical Emission Spectrometry (ICP-OES).

**Table 2:** L16 experimental design matrix

| Rotating speed (rpm) | Feed rate (L/h) | Packing density (kg/m$^3$) | Initial concentration (mg/L) | pH | S/N ratio |
|---|---|---|---|---|---|
| 400 | 20 | 153 | 50 | 2 | 9.83 |
| 400 | 30 | 255 | 100 | 3 | 26.87 |
| 400 | 40 | 357 | 150 | 4 | 26.79 |
| 400 | 50 | 510 | 200 | 5 | 28.65 |
| 800 | 20 | 255 | 150 | 5 | 27.43 |
| 800 | 30 | 153 | 200 | 4 | 26.85 |
| 800 | 40 | 510 | 50 | 3 | 29.60 |
| 800 | 50 | 357 | 100 | 2 | 25.70 |
| 1200 | 20 | 357 | 200 | 3 | 25.30 |
| 1200 | 30 | 510 | 150 | 2 | 26.45 |
| 1200 | 40 | 153 | 100 | 5 | 25.65 |
| 1200 | 50 | 255 | 50 | 4 | 28.14 |
| 1600 | 20 | 510 | 100 | 4 | 27.89 |
| 1600 | 30 | 357 | 50 | 5 | 28.12 |
| 1600 | 40 | 255 | 200 | 2 | 26.08 |
| 1600 | 50 | 153 | 150 | 3 | 29.38 |

2.3.2    Fine-tuning stage

The results of the initial optimization method could be used to reveal the significance of each factor by ranking them. The ranking was based on the delta values, which were calculated as the difference of the highest and lowest mean S/N ratio values of each factor. Depending upon the rank obtained, the most important factors influencing the removal of arsenic was selected and a fine-tuning experiment was conducted to obtain a more accurate result. The insignificant factor was kept at a constant value, as suggested by the initial optimum experiment. For the fine-tuning experiment, three significant factors were chosen, namely pH, feed rate and packing density based on the coarse optimization values and an L9 array of experiments with three different levels were utilized (Tables 3 and 4). The experiments were conducted in similar manner to the initial optimization but in this fine-tuning experiment the run time was kept at three hours to reach complete equilibrium. The percentage removal was calculated by Equation 4, where $C_0$ (mg L$^{-1}$) is the initial arsenic concentration, and $C_t$ (mg L$^{-1}$) is the arsenic concentration at any time t.

$$\text{Percentage removal}, \% = \frac{C_0 - C_t}{C_0} \times 100 \qquad (4)$$

**Table 3:** Levels of the control factors for fine tuning

| Investigating parameters | Level 1 | Level 2 | Level 3 |
|---|---|---|---|
| pH | 2 | 3 | 4 |
| Feed rate(L/h) | 40 | 45 | 50 |
| Packing density(kg/m$^3$) | 357 | 510 | 663 |

**Table 4:** L9 experimental design matrix

| pH | Feed rate (L/h) | Packing density (kg/m$^3$) |
|---|---|---|
| 2 | 40 | 357 |
| 2 | 45 | 510 |
| 2 | 50 | 663 |
| 3 | 40 | 510 |
| 3 | 45 | 663 |
| 3 | 50 | 357 |
| 4 | 40 | 663 |
| 4 | 45 | 357 |
| 4 | 50 | 510 |

# 3 Result and discussions

## 3.1 Characterization of the activated carbon

The characterization study for the activated carbon was carried out using scanning electron microscopy, Brunauer–Emmett–Teller (BET) surface area analysis and FTIR spectroscopy. The SEM image in Fig. 2 shows that the surface morphology of the activated carbon is rough and porous. Nitrogen adsorption/desorption isotherms can be used to determine the specific surface area of the activated carbon through the utilization of BET equation. The nitrogen adsorption/desorption plot shown in Fig. 3 suggests that the activated carbon can be characterized as mesoporous and microporous adsorbent (monolayer adsorption only) with relatively small external surfaces. The BET surface area was found to be 583 $m^2$/g. The pore size distribution curves show that the activated carbon contained mainly micro and meso pores which assisted in the adsorption process. The average pore diameter of the activated carbon was found to be 22 Å.
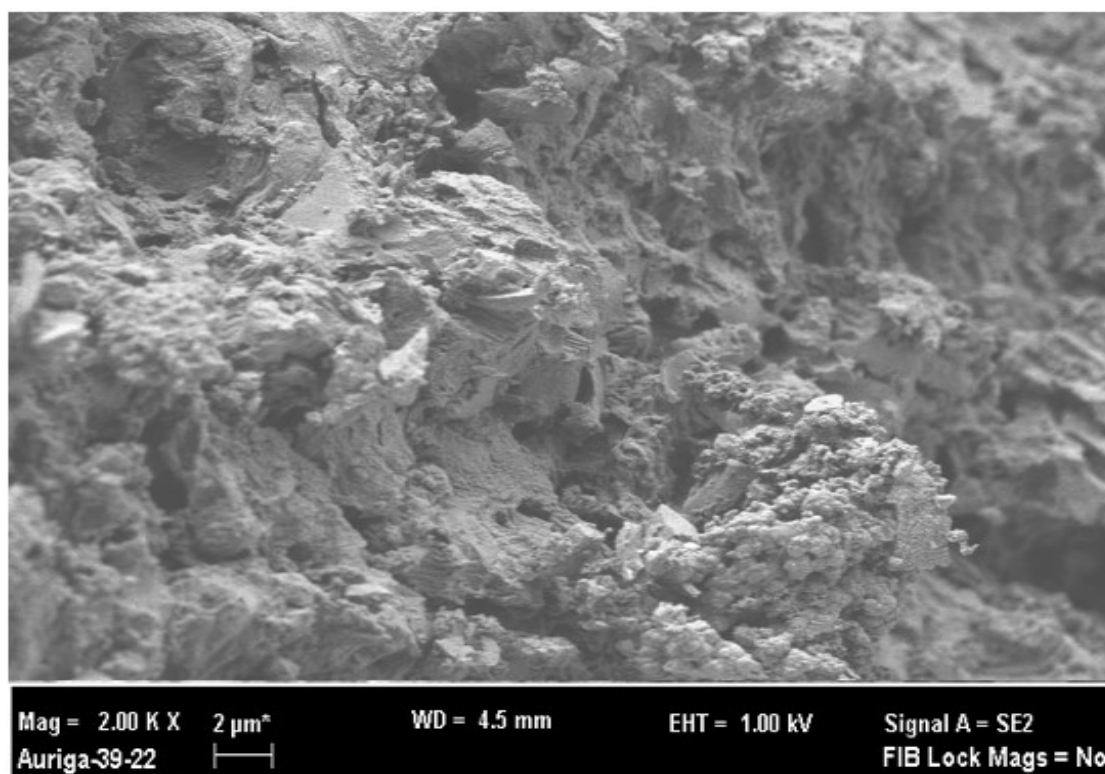


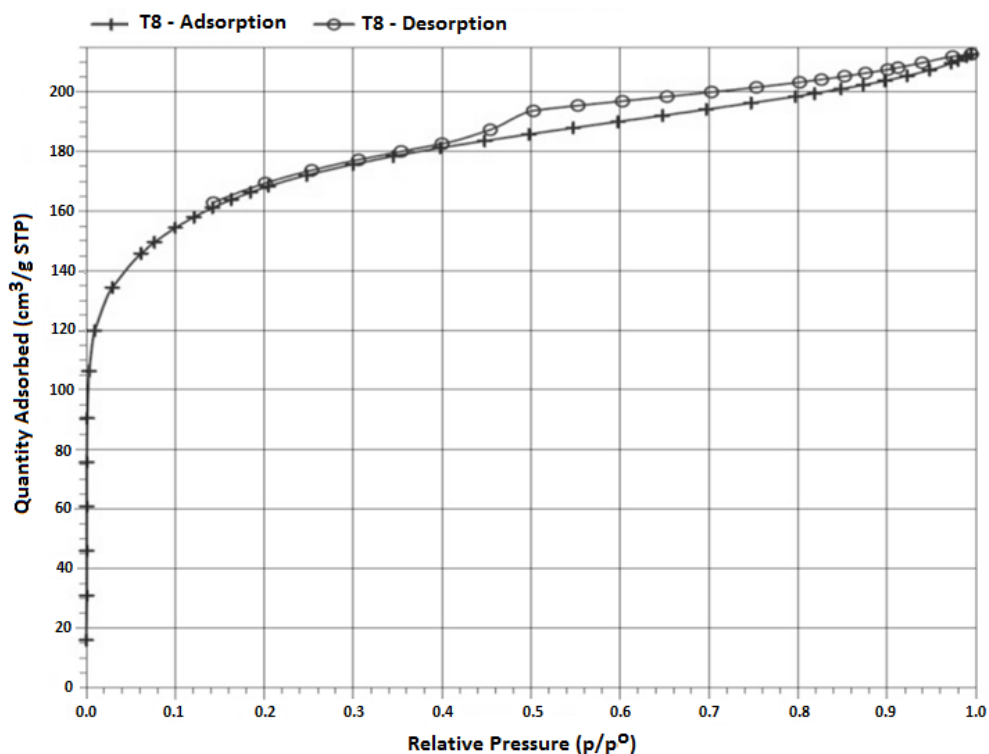**Fig. 2**: SEM image of the activated carbon

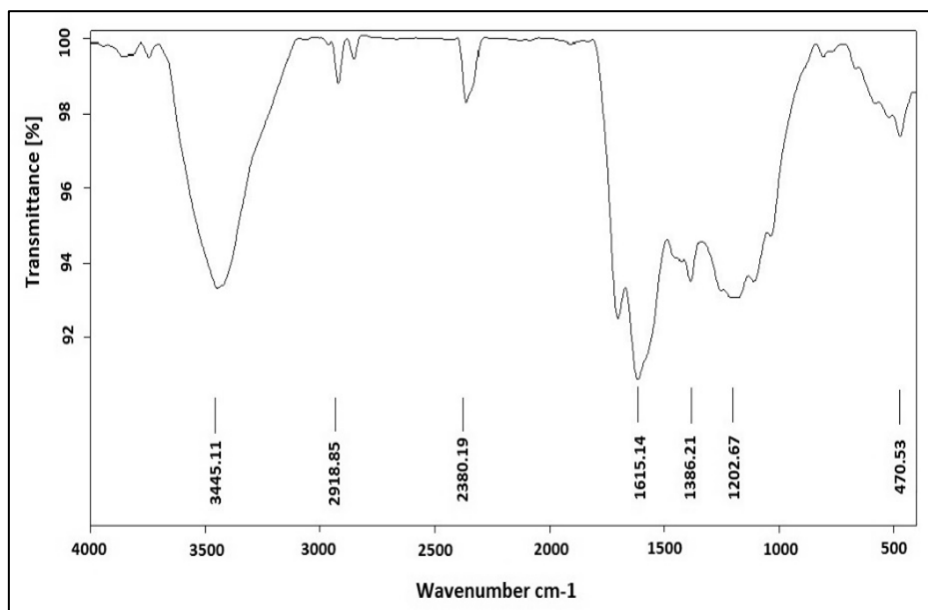**Fig. 3:** Nitrogen adsorption/desorption plot for the activated carbon.



**Fig. 4:** FT-IR image for the activated carbon.

FTIR data of the activated carbon in Fig. 4 reveals a peak between 3500-3200 cm$^{-1}$ which is attributed to O-H stretching of alcohol group or phenol group. Intensity of the band of 3000-2850 cm$^{-1}$ corresponding to C-H stretch of alkanes is minimum, suggesting these groups are not present in the activated carbon. The complex peaks around 1580-1650 cm$^{-1}$ in the activated carbon could be attributed to C-C stretch of aromatic ring and C=O axial deformation, such as highly conjugated C=O

11

stretching or C–O stretching in carboxyl groups (Shu et al., 2017). The C-O stretch for alcohol group, carboxylic acid group, ester group corresponding to the bands 1300-1000 cm$^{-1}$ is present in the activated carbon.

## 3.2 Initial optimization: Effects of the control factors on arsenic removal

A set of 16 experimental runs were performed in triplicate and the calculated S/N ratio is as given in Table 2. The main effects of the parameters on arsenic removal are as shown in the Fig. 5. It can be observed that with increasing of rotating speed from 400 rpm to 800 rpm, the S/N ratio increased. Then, as the rotating speed was increased to 1200 rpm, a slight drop in S/N ratio was observed. However, further increase in the rotating speed again resulted in an increase in the S/N ratio. The highest value of S/N ratio was obtained at level 4 which was 1600 rpm. The initial increase in S/N ratio can be attributed to the increase in mass transfer coefficient due to higher centrifugal force. The decrease in adsorption at 1200 rpm occurred due to the fact that the solid mass of activated carbon shifted towards the outer wall of the rotor with increasing rotor speed, thereby decreasing the path length of the liquid flow within activated carbon. The liquid profile inside the rotor also took an 'egg shell' like shape due to the centrifugal force (Lubarda, 2013), and therefore, contributed to the decrease in path length. With increasing rotational speed, the depth of the 'egg shell' increased and path length decreases further.  In this case, the increase in mass transfer coefficient due to increasing centrifugal force (Panda et al., 2011) cannot compensate for the effect of decrease in liquid flow path length. However, when the rotor speed was increased further, the adsorption again increased. In this case, the increase in the mass transfer coefficient predominated over the decrease in path length due to displacement of the activated carbon and the water profile towards the outer wall of the rotor (Das et al., 2008).
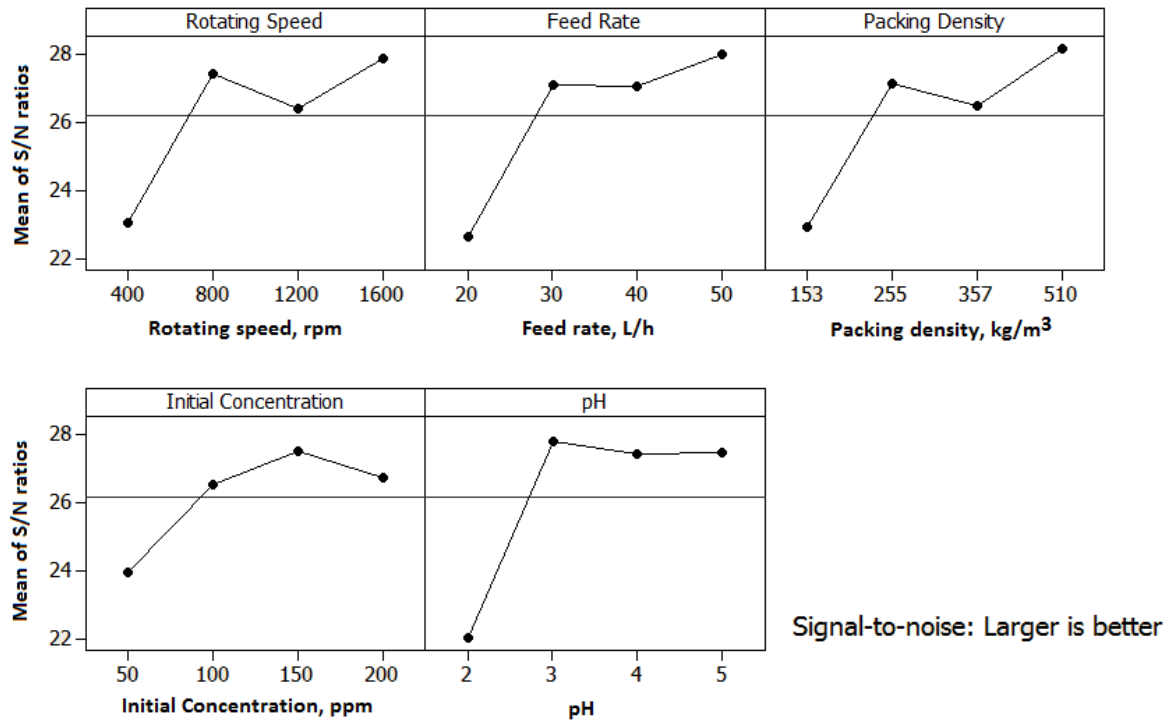
**Fig. 5:** Main effects plot for S/N in coarse optimization

Feed rate is one of the parameters that can affect the adsorption of arsenic. It was observed from Fig. 5 that there is an increasing trend in the S/N ratio with the increase in feed rate. Higher feed rate increases the probability of contact between the activated carbon and liquid, which in turn increases the adsorption of arsenic (Kundu et al., 2016). In addition, the increasing trend of S/N ratio was also observed in case of packing density. With increasing amount of activated carbon, the packing was more compact and there was less distortion of the pack during high speed rotation. This ensures that the path length travelled by the liquid was maintained high in comparison to low compaction where less quantity of activated carbon was used. The initial increasing trend of S/N ratio with increasing concentration was due to the fact that with increasing concentration more arsenic was available for adsorption. However, increase in concentration from 150 ppm to 200 ppm results in a reduced S/N ratio, as shown in Fig. 5. This was possibly due to the saturation of arsenic on the activated carbon, causing the reduction in the removal efficiency. Hence, at very high concentration, the adsorption was not feasible.

pH played a significant role in case of arsenic adsorption. It was observed that at pH of 2, the S/N ratiowas very low and it increased substantially at pH 3 and remained almost the same at pH 4

13

and pH 5. The measured redox potential of the solutions were found to be between 0.7V to 0.75V. According to the Eh-pH diagram of arsenic given in Fig. 6, the main species at pH 2 is neutral $H_3AsO_4$ and the main species at pH 3-5 is $H_2AsO_4^-$. At lower pH, the surface of the activated carbon becomes highly protonated. At pH 3, as the negatively charged arsenic species predominated, the electrostatic force of attraction between the protonated surface of activated carbon and the charged species allowed higher adsorption. The trend remained almost the same at pH 4 and 5. However, at pH 2, a very low S/N ratio was observed. It can be suggested that, at such pH, the neutral species was predominating in the solution and there were less attraction for the protonated surface, which resulted in less adsorption.
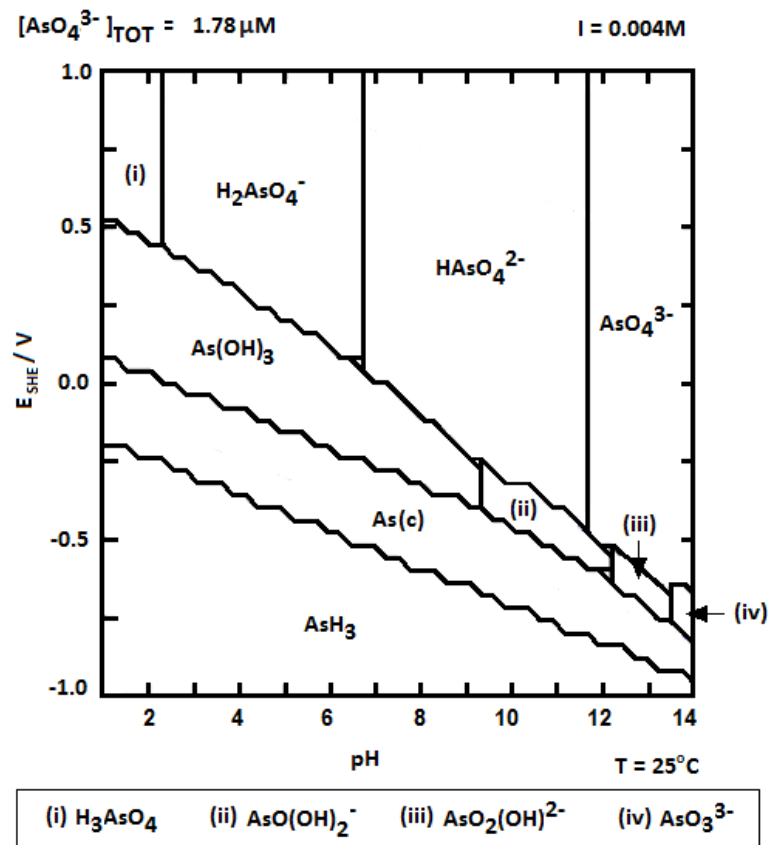


**Fig. 6:** Eh-pH diagram of arsenic species (Hoyos et al., 2013)

The initial best settings of the parameters for arsenic removal were the levels with highest S/N ratio based on the larger-the-better algorithm. The response for S/N ratio for each level is as shown in Table 5. The bold marked values indicate the highest value of S/N ratio and the corresponding levels

are the initial best settings for arsenic removal in RPB using the activated carbon. According to Table 5, the best setting is rotating speed of 1600 rpm, feed rate of 50 L/h, packing density of 510 kg/m$^3$, initial concentration of 150 ppm, and pH of 3. The significance of the parameters is measured by the difference of the highest and lowest S/N ratio across the levels, i.e. the fluctuation of the S/N ratio determines whether that parameter has significant effect on the removal or not. This difference is denoted by delta values. The higher the delta value for the factor, the more significant it is. Based on the delta values, a rank is assigned to the factors. The most significant parameter is assigned number 1 rank and subsequent ranks are provided according to the delta values. From Table 5, it is observed that the most important 3 factors are pH, feed rate and packing density.

**Table 5:** Response table for signal to noise ratios (larger is better) for coarse optimization

| Level | Rotating speed | Feed rate | Packing density | Initial concentration | pH |
|-------|----------------|-----------|-----------------|-----------------------|--------|
| 1 | 23.04 | 22.62 | 22.93 | 23.93 | 22.02 |
| 2 | 27.4 | 27.08 | 27.13 | 26.53 | **27.79** |
| 3 | 26.39 | 27.03 | 26.48 | **27.52** | 27.42 |
| 4 | **27.87** | **27.97** | **28.15** | 26.72 | 27.47 |
| **Delta** | 4.84 | 5.36 | 5.22 | 3.59 | 5.77 |
| **Rank** | 4 | 2 | 3 | 5 | 1 |

## 3.3    Fine-tuning experiment

Once the most significant factors were determined, these three factors were used to obtain more accurate levels of the parameter setting. The range of values was narrowed down to the close proximity of the initial best settings. The parameters and levels chosen for fine-tuning experiment are as shown in Table 3.
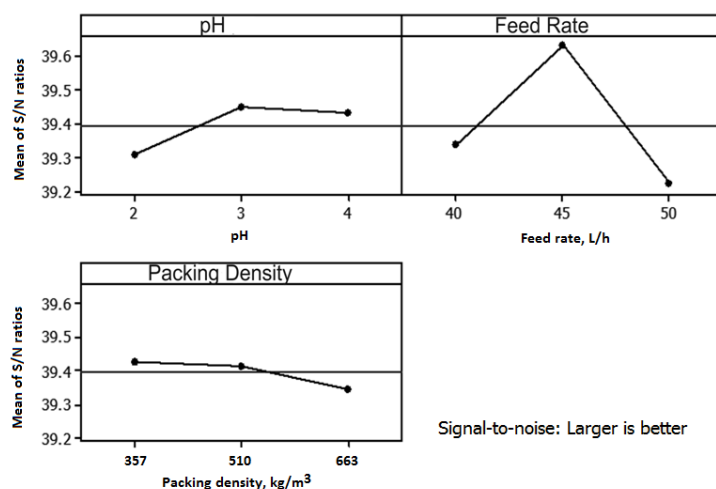
**Fig. 7:** Main effect plot for S/N ratio in the fine-tuning experiment

The L9 experiments were carried out and the obtained results suggested that the initial optimization was accurate and the fine-tuning values coincide with the initially suggested best settings. The rotating speed was fixed at 1600 rpm and the initial concentration was fixed at 50 ppm.

Fig. 7 shows the main effect plots for S/N ratio in case of the fine-tuning experiments. The highest S/N ratio was observed at level 2 for pH and level 2 for feed rate. For packing density, the S/N ratio at level 1 and level 2 are almost similar. Therefore, the fine-tuning experiment suggest that the optimised best setting for the arsenic removal in RPB is pH of 3, feed rate of 45 L/h and packing density of 357 $kg/m^3$ while the rotating speed is 1600 rpm and the initial concentration is 50 ppm. According to these fine tuning experiments, it was observed that the initial best setting was not exactly accurate. When the range was narrowed down, more accurate best settings were obtained. The reduction of feed rate from 50 L/h to 45 L/h will save energy required for pumping. Reduction of packing density is also significant as this will reduce the amount of activated carbon required, thus contributing to the reduction of operating cost. An experiment was conducted based on the suggested optimum setting and the predicted removal and actual removal coincided with each other satisfactorily, as given in Table 6.

**Table 6:** Optimum conditions obtained from fine tuning experiments at 1600 rpm and 50 ppm concentration

| pH | Feed rate (L/h) | Packing density ($kg/m^3$) | Predicted removal (%) | Observed removal (%) |
|---|---|---|---|---|
| 3 | 45 | 357 | 96.68 | 94.09 |

# 4   Conclusion

Taguchi method was applied in this study to determine the optimum operating conditions for the adsorption of arsenic on commercially available activated carbon in RPB system. The experiment was conducted in two parts. Initially, the best setting for the removal of arsenic in rotating packed bed was determined by considering a broad range of the experimental parameters, namely rotating speed, feed rate, packing density, initial concentration and initial solution pH. It was observed that feed rate, packing density and pH were the most significant factors based on the variation in their S/N values across the levels. In the fine tuning stage, the range of these three significant parameters were selected in the near vicinity of the initial best settings and the other two parameters, i.e. rotating speed and initial concentration were fixed at 1600 rpm and 50 ppm, respectively. It was observed that the optimum operating conditions became more accurate and precise when fine-tuning experiments were conducted. More accurate settings for the experiments contribute to variability in the adsorption process and reduced material and energy loss. The predicted removal of 96.68% is in very good agreement with the experimentally obtained removal of 94.09% at the best settings of the operating parameters.

## Acknowledgements

# References

Aber, S., Khataee, A., Sheydaei, M. 2009. Optimization of activated carbon fiber preparation from Kenaf using $K_2HPO_4$ as chemical activator for adsorption of phenolic compounds. *Bioresource Technology*, **100**(24), 6586-6591.

Apte, P.R. 2000. INTRODUCTION TO TAGUCHI METHOD, Vol. 2014. Retrieved on 3 May 2016, from: https://www.ee.iitb.ac.in/~apte/CV_PRA_TAGUCHI_INTRO.htm

Banerji, T., Chaudhari, S. 2016. Arsenic removal from drinking water by electrocoagulation using iron electrodes- an understanding of the process parameters. *Journal of Environmental Chemical Engineering*, **4**, 3990–4000.

Chuang, C.L., Fan, M., Xu, M., Brown, R.C., Sung, S., Saha, B. and Huang, C.P. 2005. Adsorption of arsenic(V) by activated carbon prepared from oat hulls. *Chemosphere*, **61**, 478-483.

Das, A., Bhowal, A., Datta, S. 2008. Continuous biosorption in rotating packed-bed contactor. *Industrial & Engineering Chemistry Research*, **47**(12), 4230-4235.

Durán-Jiménez, G., Hernández-Montoya, V., Montes-Morán, M.A., Bonilla-Petriciolet, A., Rangel-Vázquez, N.A. 2014. Adsorption of dyes with different molecular properties on activated carbons prepared from lignocellulosic wastes by Taguchi method. *Microporous and Mesoporous Materials*, **199**(0), 99-107.

Gupta, S.K. and Chen, K.Y. 1978. Arsenic removal by adsorption. *Journal of the Water Pollution Control Federation*, **50**, 493–506

Kobya, M., Ulu, F., Gebologlu, U., Demirbas, E., Oncel, M.S. 2011. Treatment of potable water containing low concentration of arsenic with electrocoagulation: Different connection modes and Fe-Al electrodes. *Separation and Purification Technology*, **77**, 283–293.

Korte, N.E. and Fernando, Q. 1991. A review of arsenic (III) in groundwater. *Critical Reviews in Environmental Science and Technology*, **21(1),** 1–39.

Kundu, A., Shakira Hassan, L., Redzwan, G., Robinson, D., Ali Hashim, M., SenGupta, B. 2016. Application of a rotating packed bed contactor for removal of Direct Red 23 by adsorption. *Desalination and Water Treatment*, **57**(29), 13518-13526.

Li, K., Zheng, Z., Li, Y. 2010. Characterization and lead adsorption properties of activated carbons prepared from cotton stalk by one-step $H_3PO_4$ activation. *Journal of Hazardous Materials*, **181**(1–3), 440-447.

Lin, C.-C., Liu, H.-S. 1999. Adsorption in a centrifugal field: Basic dye adsorption by activated carbon. *Industrial & Engineering Chemistry Research*, **39**(1), 161-167.

Lubarda, V. 2013. The shape of a liquid surface in a uniformly rotating cylinder in the presence of surface tension. *Acta Mechanica*, **224**(7), 1365-1382.

Malwal. D., Gopinath, P. 2017. Silica stabilized magnetic-chitosan beads for removal of arsenic from water. *Colloid and Interface Science Communications*, **19**, 14–19.

Mondal, P., Mohanty, B., Majumder, C.B. 2013. Effect of pH and Treatment Time on the Removal of Arsenic Species from Simulated Groundwater by Using $Fe^{3+}$ and $Ca^{2+}$ Impregnated Granular Activated Charcoals. *Chemical Engineering and Science*, **1(2)**, 27-31.

Nistico, R., Celi, L.R., Prevot, A.B., Carlos, L., Magnacca, G., Zanzo, El., Martin, M. 2018. Sustainable magnet-responsive nanomaterials for the removal of arsenic from contaminated water. *Journal of Hazardous Materials*, **342**, 260–269.

Ortega, A., Oliva, I., Contreras, K.E., Gonzalez, I., Cruz-Diaz, M.R., Rivero, E.P. 2017. Arsenic removal from water by hybrid electro-regenerated anion exchange resin/electrodialysis process. *Separation and Purification Technology*, **184**, 319–326.

Panda, M., Bhowal, A., Datta, S. 2011. Removal of hexavalent chromium by biosorption process in rotating packed bed. *Environmental Science & Technology*, **45**(19), 8460-8466.

Ramshaw, C., Mallinson, R.H. 1981. Mass Transfer Process, (Ed.) U.S. Patent, Vol. 4,283,255. USA.

Ratnaike, R.N. 2003. Acute and chronic arsenic toxicity. *Postgraduate Medical Journal*, **79**, 391-396.

Roghani, M., Nakhli, S.A.A., Aghajani, M., Rostami, M.H., Borghei, S.M. 2016. Adsorption and oxidation study on arsenite removal from aqueous solutions by polyaniline/polyvinyl alcohol composite. *Journal of Water Process Engineering*, **14**, 101–107.

Shankar, S., Shanker, U., Shikha. 2014. Arsenic contamination of groundwater: A review of sources, prevalence, health risks, and strategies for mitigation. *The Scientific World Journal*, **2014**, 1-18

Shu, J., Cheng, S., Xia, H., Zhang, L., Peng, J., Li, C., Zhang, S. 2017. Copper loaded on activated carbon as an efficient adsorbent for removal of methylene blue. *RSC Advances*, **7**, 14395-14405.

Hoyos, S.E.G., Flores, M.A., Gonzalez, A.R., Fajardo, C.G., Zoloeta, S.C., Orozco, H.V. 2013. Comparing two operating configurations in a full-scale arsenic removal plant. Case study: Guatemala. *Water*, **5**(2), 834-851.

Stankiewicz, A.I., Moulijn, J.A. 2000. Process intensification: transforming chemical engineering. *Chemical Engineering Progress*, **96**(1), 22-34.

Taguchi, G. 1986. *Introduction to quality engineering : designing quality into products and processes.* Asian Productivity Organization, Tokyo.

USEPA, 2017. *Drinking Water Requirements for States and Public Water Systems*. Retrieved 23 January 2018, from https://www.epa.gov/dwreginfo/chemical-contaminant-rules.

Vieira, B.R.C., Pintor, A.M.A., Boaventura, R.A.R., Botelho, C.M.S., Santos, S.C.R. 2017. Arsenic removal from water using iron-coated seaweeds. *Journal of Environmental Management*, **192**, 224-233.

Wang, G.Q., Xu, Z.C., Yu, Y.L., Ji, J.B. 2008. Performance of a rotating zigzag bed—A new HIGEE. *Chemical Engineering and Processing: Process Intensification*, **47**(12), 2131-2139.

Wang, S., Gao, B., Zimmerman, A.R., Li, Y., Ma, L., Harris, W.G., Migliaccio, K.W. 2015. Removal of arsenic by magnetic biochar prepared from pinewood and natural hematite. *Bioresource Technology*, **175**, 391-395.

Wei, Z., Liang, K., Wu, Y., Zou, Y., Zuo, J., Arriagada, D.C., Pan, Z., Hu, G. 2016. The effect of pH on the adsorption of arsenic(III) and arsenic(V) at the $TiO_2$ anatase [101] surface. *Journal of Colloid and Interface Science*, **462**, 252-259